ORIGINAL ARTICLE

Nucleation and polymorphism of *trans*-1,4-polyisoprene containing copper phthalocyanine

Tomoya Tsuboi, Masashi Harada, Kei Ishii, Susumu Fujiwara and Takashi Itoh

The effect of α- or β-copper phthalocyanine (CuPc) as a nucleating agent during the crystallization of *trans*-1,4-polyisoprene (TPI) was evaluated using polarized optical microscopy (POM), differential scanning calorimetry (DSC) and wide angle X-ray diffraction (WAXD). Pure TPI crystallizes into either a high-melting crystal form (HMF) or a low-melting crystal form (LMF), depending on the cooling condition of the melt. The HMF melts at ∼60 °C and LMF typically melts at ∼50 °C. Observation by POM showed that the LMF is generated at the interface between TPI and either α- or β-CuPc, selectively, when crystallized at 38 °C. In DSC measurements, the TPI composites containing α- or β-CuPc showed a higher crystallization temperature than that of pure TPI during the melt cooling process. Such results provided evidence that the α- or β-CuPc acted as a nucleating agent for TPI. The data obtained from WAXD proved that the HMF was generated mainly when pure TPI was cooled from the melt at a rate of 5 °C min⁻¹, while the LMF was generated predominantly when the TPI/α- or β-CuPc composites were crystallized under the same cooling conditions as those used for pure TPI. These results led to the conclusion that α- and β-CuPc acted as phase selective nucleating agents for LMF-TPI.

INTRODUCTION

Gutta-percha or *trans*-1,4-polyisoprene (TPI) has long been known to be a bio-based polymer.[1,2] Although it has been used as a tooth canal-filling material or a golf ball covering, it has been given less attention than other biopolymers, for example, polylactic acid or poly-hydroxybutylate. Recently, green and sustainable chemistry has become more important, and TPI is being reevaluated. Bulk TPI is a crystalline polymer, and it generally crystallizes in two forms from the melt: α-form and β-form. The α- and β-forms of TPI crystals are often called the high-melting crystal form (HMF) and low-melting crystal form (LMF), respectively.[3] The HMF is obtained by slow-cooling from the melt, whereas the LMF is obtained by rapid-cooling, or quenching, from the melt. The fundamental properties of TPI, such as crystal morphology or crystallization behavior, have been studied by Davies and Long[4,5] However, the properties of TPI composites containing additives have been comparatively less well-studied.[6]

Additives are often used to enhance the physical properties of polymers. Among the additives, nucleating agents accelerate the crystallization rate or change the crystal structures of crystalline polymers.[7] For example, copper phthalocyanine (CuPc) acts as a nucleating agent for polylactic acid or polypropylene and effectively promotes the crystallization of the polymers.[8,9] *Trans*-quinacridone promotes the generation of the β-crystal of polypropylene.[10] Recently, Vijayakumar *et al.*[11] have reported that onium salts act as a β-form

nucleating agent for poly(vinylidene fluoride). Acceleration or phase control via polymer crystallization has received significant industrial and academic interest, so the nucleating agents of polymers have been studied extensively.

The effect of nucleating agents on TPI crystallization was investigated in this report. As a nucleating agent, CuPc was chosen because it shows a strong nucleating effect for several polymers, as mentioned above. CuPc is a type of blue pigment and is known to have several crystalline forms (for example, α, β, γ, δ and ε).[12] Among them, the metastable α-form CuPc (α-CuPc) and stable β-form CuPc (β-CuPc) have been used widely. In this report, the crystallization behaviors of TPI/α-CuPc and TPI/β-CuPc composites were observed by polarized optical microscopy (POM). The crystallization and melting behaviors of TPI containing either α-CuPc or β-CuPc were examined by differential scanning calorimetry (DSC). The wide angle X-ray diffraction (WAXD) method was used to analyze the crystal structure of the composites.

EXPERIMENTAL PROCEDURE

The materials were commercially available and used without further purification. The TPI was purchased from Scientific Polymer Products, Inc. (Ontario, NY, USA). The Mn of the TPI is 92 000, and the Mw of the TPI is 400 000 with a Mw/Mn value of 4.35.

Powders of α- and β-CuPc were purchased from Tokyo Chemical Industry Co., Ltd. (Tokyo, Japan). The crystallite sizes of α-CuPc, measured by

Department of Macromolecular Science and Engineering, Kyoto Institute of Technology, Kyoto, Japan
Correspondence: T Tsuboi, Department of Macromolecular Science and Engineering, Kyoto Institute of Technology, Matsugasaki, Sakyo-ku, Kyoto 606-8585, Japan.
E-mail: tsuboi.tomoya@kao.co.jp

916

half-widths on WAXD diffraction, were 72–128 nm, and those of β-CuPc were 133–318 nm.

POM observation was performed using a laser microscope VHX-1000 by Keyence (Osaka, Japan) with a microscope hot stage LK300B by Linkam (Tadworth, UK). Samples for the POM observation were prepared by pressing TPI with 0.01 wt% of either α- or β-CuPc powder between two cover glasses. The POM observations were carried out in the space surrounding the powder. The Linkam LK300B consists of two adjacent heating stages. One stage was set at 100 °C, and the other was set at 38 °C. After a sample was held at 100 °C for 10 min to erase the thermal history completely, the sample was quickly moved to the other stage, and the crystallization process of the sample was observed by POM.

The composites for DSC and WAXD measurements were prepared as follows. The polymer and 1 wt% of α- or β-CuPc were mixed and melted at 100 °C using a hot press machine. After cooling to room temperature, the thin sheet composites were cut into small pieces. These pieces were put together and melted at 100 °C again in a hot press machine. This process was repeated until the powders were dispersed uniformly in the TPI. Pure TPI sheets were prepared as a reference sample via the same procedure. Pure TPI, the TPI/α-CuPc composite and the TPI/β-CuPc composite are hereafter referred to as TPI-0, TPI-1 and TPI-2, respectively.

The thermal analysis was carried out using a SII differential scanning calorimeter DSC220C by Seiko Instruments Inc. (Chiba, Japan) under a nitrogen atmosphere, where the temperature was calibrated using the melting points of indium and zinc. The sample weights were 5–7 mg. Samples of TPI-0, TPI-1 and TPI-2 were heated from 25 °C to 100 °C at a rate of 5 °C min^{-1} and kept at 100 °C for 10 min to erase the thermal history and were then cooled to 0 °C at a rate of 5 °C min^{-1}. Subsequently, the samples were kept at 0 °C for 10 min and heated to 100 °C at a rate of 5 °C min^{-1}. The DSC curves of the samples during the cooling and subsequent heating processes were recorded.

The WAXD measurement was performed using a MAC Science M18XHF22 with Ni-filtered CuKα radiation. Thin films of TPI-0, TPI-1 and TPI-2 were prepared by cooling at a rate of 5 °C min^{-1} from 100 °C in DSC. As reference samples, two types of thin films of TPI-0 were prepared: one was cooled slowly at a rate of 0.17 °C min^{-1} from the melt, and the other was cooled rapidly with liquid nitrogen from 100 °C. The WAXD photographs of these samples were taken at 25 °C.

RESULTS AND DISCUSSION
POM observation

The α- or β-CuPc powder was dispersed in ethanol, and the particle sizes were measured by the laser diffraction technique using a LA-950 by HORIBA, Ltd. (Kyoto, Japan). The median and average sizes of α-CuPc were 5.92 μm and 9.68 μm, respectively. The median and average sizes of β-CuPc were 27.48 and 27.14 μm, respectively.

Samples prepared by pressing TPI and powder of α-CuPc or β-CuPc were observed with POM. Figures 1a and b show TPI with α-CuPc and TPI with β-CuPc observed with POM at 100 °C. The black particles in the figures are α-CuPc or β-CuPc. TPI was in an amorphous state, and no TPI crystal was observed.
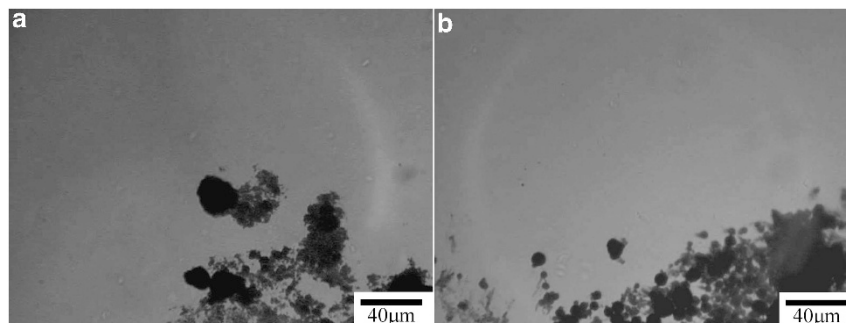
Figures 2a and b show TPI with α-CuPc and TPI with β-CuPc, respectively, both kept at 38 °C for 5 min. In both figures, the TPI crystal looks different in the regions away from the CuPc particles than it does near the particles. The crystals around CuPc do not appear spherulitic and seem to be generated along the surface of CuPc particles. These observations indicate that these crystals grew on CuPc crystal surfaces, meaning that the α- or β-CuPc acted as a nucleating agent for the TPI crystal.

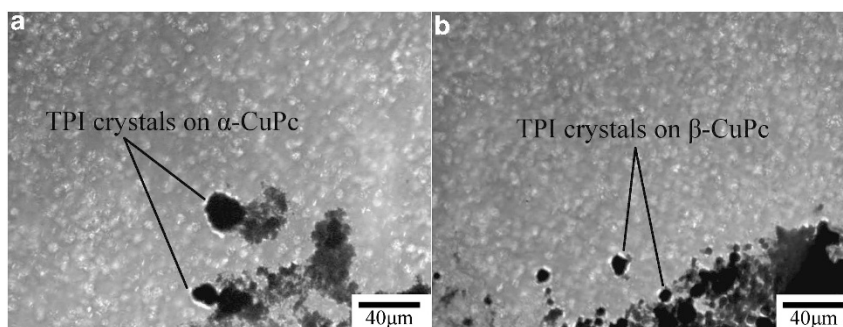Figures 3a and b are micrographs of the samples after being heated to 50 °C. At 50 °C, the crystals at the interface between TPI and α- or β-CuPc melted, and the crystals (spherulites) away from the CuPc remained. This result indicates that the crystals at the interface were the LMF and that the crystals away from CuPc were the HMF. The melting point of TPI crystals at the interface (LMF) was 50 °C, and the melting point of TPI crystals in Figure 3 (HMF) was 62 °C. These results suggest that α- or β-CuPc acted selectively as a nucleating agent for LMF-TPI.

DSC measurement

Figure 4 shows the DSC curves of TPI-0, TPI-1 and TPI-2 through the cooling process from the melt, which occurred at a rate of 5 °C min^{-1}. Exothermal peaks in the DSC curves were due to the crystallization of TPI. The peak temperatures of the crystallization exothermal curves and the crystallization enthalpies of the samples are summarized in Table 1. The crystallization temperatures of TPI-1 and TPI-2 are greater than that of TPI-0, indicating that α- or β-CuPc acted as nucleating agents and accelerated the crystallization of TPI. The amount of α- or β-CuPc in the DSC samples was much larger than that in the POM samples, and the nucleating effect of the DSC samples was much stronger than that of the POM samples. The peak temperature of the crystallization exothermal curve for TPI-0 was 24.9 °C, while those of TPI-1 and TPI-2 were 30.6 °C and 34.6 °C, respectively. The sample of TPI-2 showed the highest crystallization temperature among the samples.

Figure 5 shows the DSC curves of TPI-0, TPI-1 and TPI-2 through the heating process, which occurred at a rate of 5 °C min^{-1}, originating at 0 °C. The endothermal peaks in the DSC curves were due to the melting of the TPI crystal. The peak melting temperatures and melting enthalpies of the samples are summarized in Table 2. In this process, TPI-0 showed a minor peak at 50.6 °C and a major peak at 60.8 °C. TPI-1 showed split peaks at 46.7 °C and 50.8 °C and a small peak at 60.3 °C. TPI-2 showed a single peak at 50.9 °C. The melting point of the TPI-0 crystal was the highest among the samples. The samples containing α- or β-CuPc showed lower melting points.

The crystalline form of pure TPI obtained through the melt crystallization changes depending on the cooling process (either the

Figure 1 Polarized optical micrographs of (a) TPI/α-CuPc and (b) TPI/β-CuPc held at 100 °C for 10 min.

Figure 2 Polarized optical micrographs of (**a**) TPI/α-CuPc and (**b**) TPI/β-CuPc held at 38 °C for 5 min.
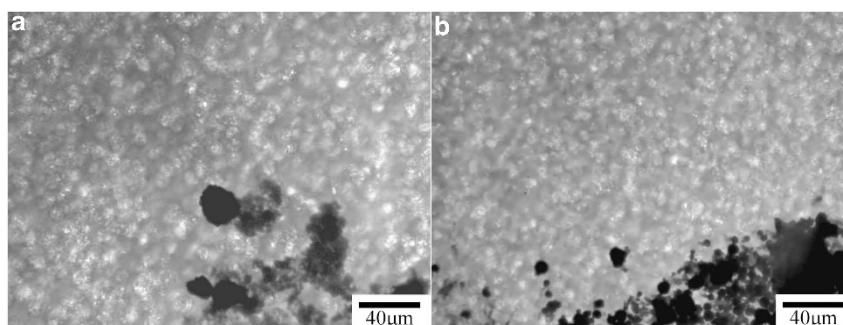
Figure 3 Polarized optical micrographs of (**a**) TPI/α-CuPc and (**b**) TPI/β-CuPc heated to 50 °C.
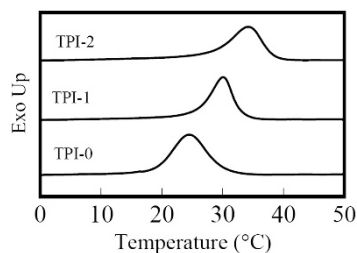
Figure 4 DSC curves of three samples of the cooling process from the melt occurring at a rate of 5 °C min^{-1}.
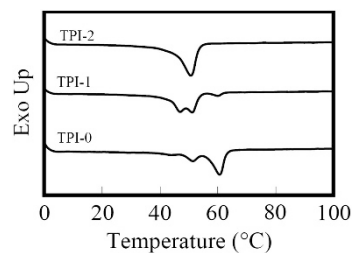

Figure 5 DSC curves of three samples of the heating process from 0 °C occurring at a rate of 5 °C min^{-1}.

Table 1 Peak temperature of crystallization (T_c) and crystallization enthalpy (ΔH_c) of three samples

Sample	T_c (°C)	ΔH_c (Jg^{-1})
TPI-0	24.9	44.8
TPI-1	30.6	38.2
TPI-2	34.6	38.0

Abbreviation: TPI, *trans*-1,4-polyisoprene.

Table 2 Peak temperature of melting ($T_{m\ low}$ and $T_{m\ high}$) and melting enthalpy ($\Delta H_{m\ low}$ and $\Delta H_{m\ high}$) of three samples

Sample	$T_{m\ low}$ (°C)	$\Delta H_{m\ low}$ (Jg^{-1})	$T_{m\ high}$ (°C)	$\Delta H_{m\ high}$ (Jg^{-1})
TPI-0	50.6	9.0	60.8	32.1
TPI-1	46.7, 50.8	38.6	60.3	2.3
TPI-2	50.9	43.7		

Abbreviation: TPI, *trans*-1,4-polyisoprene.

HMF or LMF).[1] The HMF is generated by slow cooling, and the LMF is obtained by rapid cooling. The melting points of the HMF and LMF samples were 62 °C and 50 °C, respectively, according to microscopic observation; thus, the TPI-0 crystals were considered to be primarily the HMF and the TPI-1 and TPI-2 crystals were considered to be primarily the LMF. The endothermal peak at

46.7 °C observed for TPI-1 may be the melting of the incomplete LMF crystal. The slight peak at ∼45 °C observed in the TPI-0 sample is also considered to be the melting of the LMF. The samples for the POM observation were made by pressing TPI with a small amount of the CuPc powder to observe the interfaces between the TPI and CuPc. In Figure 2, TPI crystals away from CuPc were of the HMF

variety and remained at 50 °C. Conversely, the samples for the DSC measurement contained 1 wt% CuPc, and the CuPc was dispersed more uniformly in the TPI matrix by sequential pressing. The contact area between the TPI and CuPc of the DSC samples was much larger than that of the POM samples.

At a glance, it may look unreasonable that the pure TPI has a lower crystallization temperature and a higher melting point. The melting point and crystallization temperature are closely related, but they are not the same. The crystallization process consists of the nucleation and growth of a crystal. In the cooling process, the nucleus of the LMF crystal could not be formed in pure TPI at a high temperature ($\sim$30 °C). However, for the TPI/CuPc composites, the LMF crystal could be generated at and grow around a nucleating agent. In the heating process, the HMF may be more stable than the LMF, and the LMF, therefore, melts earlier than the HMF. A nucleating agent may influence only the initial crystallization process and hardly influence the energy stabilization or the melting process of the formed crystal. As a result, the melting point of the LMF crystal is lower than that of the HMF crystal.

As the LMF crystal is considered to be less stable than the HMF crystal at low temperatures, the LMF may be generated because of a kinetic advantage at low temperature.[3] Through the addition of nucleating agents, the nucleus of the LMF may be energetically stabilized and the formation of the LMF may occur before the formation of the HMF. These results are consistent with the microscopy observations. Moreover, either α- or β-CuPc small particles have a large surface area due to their morphology, which effectively increases the probability and/or effect of the nucleation of the LMF-TPI.

WAXD observation

The WAXD results were examined to confirm the crystal structures of the samples generated through the DSC operation described previously. Figure 6 shows the WAXD patterns of (a) α-CuPc, (b) β–CuPc, (c) TPI cooled from the melt at a rate of 0.17 °C min^{-1} and (d) TPI cooled from the melt rapidly using liquid nitrogen.

The lattice parameters of the α-CuPc crystal are $a = 25.92$ Å, $b = 3.79$ Å, $c = 23.92$ Å, $\beta = 90.4°$ (C 2/c, monoclinic).[13] The
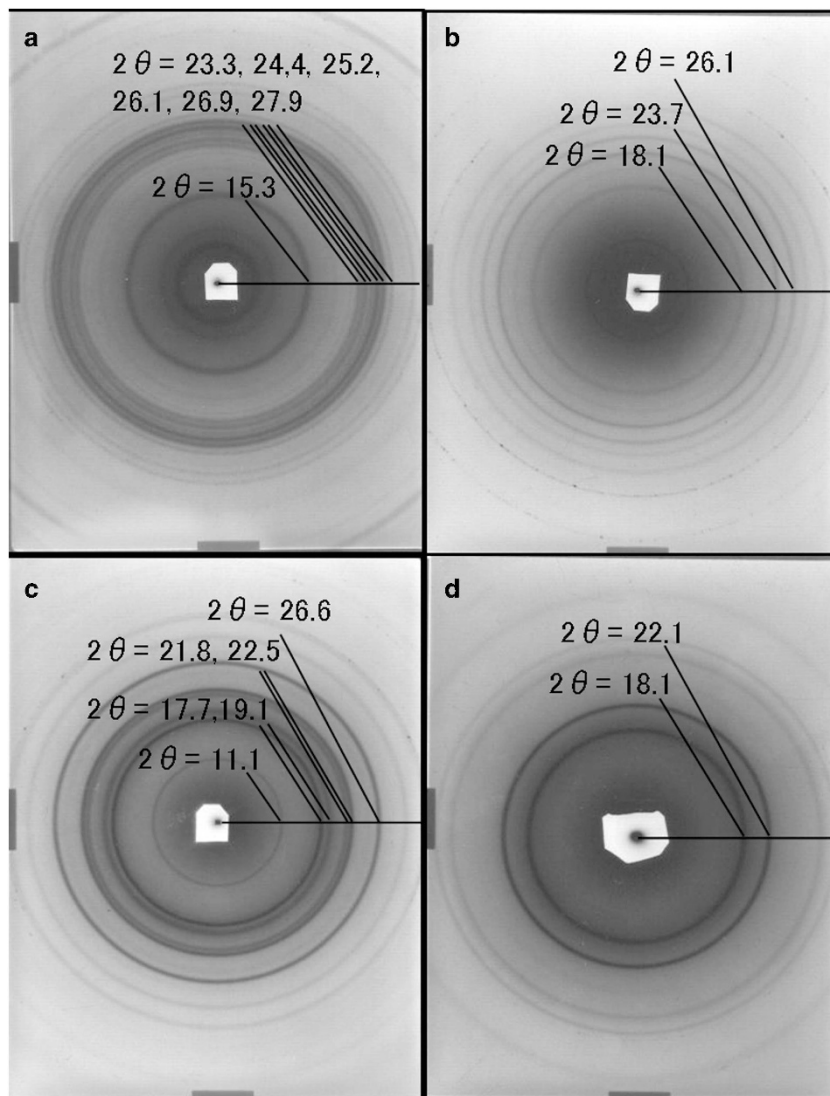
Figure 6 WAXD patterns of (**a**) α-CuPc, (**b**) β-CuPc, (**c**) TPI-0 cooled from the melt at a rate of 0.17 °C min^{-1} and (**d**) TPI-0 rapidly cooled from the melt with liquid nitrogen.

observed peaks of α-CuPc are $2\theta = 15.3°$ ($d = 5.8$ Å), $23.3°$ ($d = 3.8$ Å), $24.4°$ ($d = 3.7$ Å), $25.2°$ ($d = 3.5$ Å), $26.1°$ ($d = 3.4$ Å), $26.9°$ ($d = 3.3$ Å) and $27.9°$ ($d = 3.2$ Å), where θ is the Bragg angle, corresponding to the 402, 110, 11-1-1, 11-2-2, 11-3-3, 312 and 313 reflections of the α-CuPc crystal, respectively. The lattice parameters of the β-CuPc crystal are $a = 19.41$ Å, $b = 4.79$ Å, $c = 14.63$ Å and $\beta = 120.56°$ ($P\ 2_1/a$, monoclinic).[14–15] The observed peaks of β-CuPc are $2\theta = 18.1°$ ($d = 4.90$), $23.7°$ ($d = 3.75$ Å), and $26.1°$ ($d = 3.41$ Å), corresponding to the 011, 112 and -3-311 reflections of the β-CuPc crystal, respectively.

The lattice parameters of the HMF-TPI crystal are $a = 7.98$ Å, $b = 6.29$ Å, $c = 8.77$ Å and $\beta = 102°$ ($P\ 2_1/c$, monoclinic; reported by Takahashi et al.[16]), and those of the LMF-TPI crystal are $a = 7.78$ Å, $b = 11.78$ Å and $c = 4.72$ Å ($P\ 2_12_12_1$, orthorhombic; reported by Bunn[1]). The WAXD pattern of TPI crystallized at a rate of $0.17\ °C\,min^{-1}$ was successfully indexed as TPI-HMF. The sample had peaks at $2\theta = 11.1°$ ($d = 7.95$ Å), $17.7°$ ($d = 5.00$ Å), $19.1°$ ($d = 4.64$ Å), $21.8°$ ($d = 4.08$ Å), $22.5°$ ($d = 3.96$ Å), and $26.6°$ ($d = 3.36$ Å), which correspond to the 100, 011, 110, 111, 200 and 210 reflections of the HMF-TPI crystal, respectively. In the same way, the WAXD pattern of TPI cooled from the melt using liquid nitrogen was indexed. This pattern had peaks at $2\theta = 18.1°$ ($d = 4.90$) and $22.1°$ ($d = 4.02$ Å), corresponding to the 001 and 101 reflections of the LMF-TPI crystal, respectively. Although the shapes of the diffraction patterns of the LMF and HMF-TPI crystals were similar, the patterns of the HMF crystal showed an intense peak at $2\theta = 26.6°$.

The lattice parameters of the α-CuPc, β-CuPc, HMF-TPI and LMF-TPI crystals are summarized in Table 3.

Figure 7 shows the WAXD patterns of the (a) TPI-0, (b) TPI-1 and (c) TPI-2 crystals cooled from the melt at a rate of $5\ °C\,min^{-1}$. TPI-0 showed peaks at $2\theta = 11.3°$ ($d = 7.82$ Å), $17.9°$ ($d = 4.96$ Å), $18.8°$ ($d = 4.73$ Å) and $22.8°$ ($d = 3.90$ Å), and $26.9°$ ($d = 3.32$ Å). These peaks correspond to the 100 (HMF), 011 (HMF), 110 (HMF) or 001 (LMF), 200 (HMF) or 200 (LMF), and 210 (HMF) reflections, respectively, of TPI crystals. This pattern had a large peak at $2\theta = 26.9°$ and the sample predominantly consisted of the HMF-TPI crystal. According to the DSC observation, it was suggested that the sample is mainly composed of the HMF and contains a small amount of the LMF. The WAXD result is consistent with the DSC observations.

Figure 7b (TPI-1) shows major peaks at $2\theta = 18.6°$ ($d = 4.77$ Å), $22.5°$ ($d = 3.96$ Å), and a small peak at $26.3°$ ($d = 3.39$ Å), corresponding to the 001 (LMF), 200 (LMF) and 210 (HMF) reflections of TPI crystal, respectively. According to the DSC observations, the sample is predominantly LMF and likely contains a small amount of HMF crystallization. The small peak at $2\theta = 26.3°$ is derived from the HMF crystal.

Figure 7c (TPI-2) shows peaks at $2\theta = 18.6°$ ($d = 4.77$ Å) and $22.6°$ ($d = 3.93$ Å), corresponding to 120 (LMF) and 200 (LMF), respectively. This sample did not show any reflection from the HMF-TPI, which is consistent with the DSC observations. These results indicate that the nucleating effect of β-CuPc for the LMF-TPI crystal is stronger than that of α-CuPc. The WAXD observation proved that α- and β-CuPc promoted the crystallization of LMF-TPI, while providing no effect on HMF-TPI crystallization.

The mechanism underlying these results is unclear, but we considered an epitaxial effect as an explanation. The possibility of epitaxial crystallization is suggested by the occurrence of the lattice matching between the polymer crystal and the substrate crystal.[17–19] Consider the following lattice parameters: $c = 23.92$ Å for α-CuPc and $b = 11.78$ Å for LMF-TPI. The c value for α-CuPc is about twice the b value for LMF-TPI, and the mismatch factor is 1.5%. Similarly, the $b = 4.79$ Å for β-CuPc and the $c = 4.72$ Å for LMF-TPI are close, with a mismatch factor of 1.5%. Such small lattice mismatches may stabilize the nuclei of the LMF-TPI and promote the crystallization of the polymer. More experiments will be performed in the future to clarify the mechanism underlying these similarities.
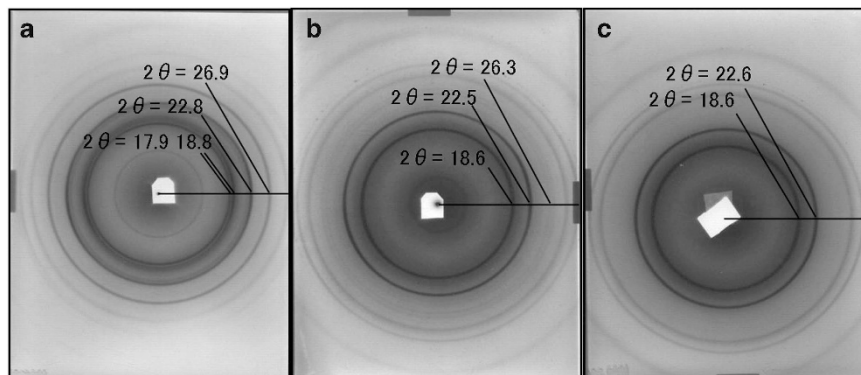
Conclusions

The crystallization behaviors of TPI containing α- or β-CuPc were investigated in comparison with those of pure TPI. The POM observation indicated that the addition of α- or β-CuPc selectively promoted crystallization of the LMF-TPI. At the interface of TPI/α- or β-CuPc, the formation of LMF-TPI was observed. As heterogeneous nucleating agents, α- and β-CuPc promoted the nucleation of LMF-TPI. The DSC measurement showed that the addition of α- or β-CuPc increased the crystallization temperature

Table 3 Lattice parameters of HMF-TPI, LMF-TPI, α-CuPc and β-CuPc

Sample	a (Å)	b (Å)	c (Å)	β (°)	Symmetry group/crystal system
HMF-TPI[16]	7.98	6.29	8.77	102	$P\ 2_1/c$/monoclinic
LMF-TPI[1]	7.78	11.78	4.72	90.0	$P\ 2_12_12_1$/orthorhombic
α-CuPc[13]	25.92	3.79	23.92	90.4	$C\ 2/c$/monoclinic
β-CuPc[14]	19.41	4.79	14.63	120.56	$P\ 2_1/a$/monoclinic

Abbreviations: CuPc, copper phthalocyanine; HMF, high-melting crystal form; LMF, low-melting crystal form; TPI, trans-1,4-polyisoprene.
The data in the table were cited from the references.

Figure 7 WAXD patterns of (a) TPI-0, (b) TPI-1, and (c) TPI-2 cooled from the melt at a rate of $5\ °C\,min^{-1}$.

and decreased the melting point. The WAXD results confirmed that the TPI/α-CuPc or TPI/β-CuPc contained LMF-TPI predominantly, if not exclusively. The precise mechanism of how α-CuPc or β-CuPc selectively promotes the nucleation of LMF-TPI crystals is still unclear, and analysis at the single crystal level is likely to be required to identify the mechanism.

1 Bunn, W. C. Molecular structure and rubber-like elasticity I. The crystal structures of β gutta-percha, rubber and polychloroprene. *Proc. R. Soc. Lond. A* **180,** 40–66 (1942).
2 Kent, E. G. & Swinney, F. B. Properties and applications of *trans*-1,4-polyisoprene. *Ind. Eng. Chem. Prod. Res. Dev.* **5,** 134–138 (1966).
3 Fischer, E. & Henderson, J. F. Study of crystallization kinetics of *trans*-1,4-polyisoprene. *J. Polym. Sci. A* **5,** 377–390 (1967).
4 Davies, C. K. L. & Long, O. E. Morphology of *trans*-1,4- polyisoprene crystallized in thin films. *J. Mat. Sci.* **12,** 2165–2183 (1977).
5 Davies, C. K. L. & Long, O. E. Kinetics of crystallization of trans-1,4-polyisoprene crystallized in thin films. *J. Mat. Sci.* **14,** 2529–2536 (1979).
6 Arvanitoyannis, I. & Blanshard, J. M. V. Crystallization kinetics of native (pure) and commercial gutta-percha (trans-polyisoprene) and the influence of metal salts, oxides, 'Thermoplast' and colouring agents on its crystallization rate. *Polym. Int.* **27,** 297–303 (1992).
7 Fairgrieve, S. *Nucleating Agents* (Smithers Rapra Technology, UK, 2007).
8 Sato, N., Fujihira, Y., Yamada, S. & Noguchi, T. Polylactic acid mold with heat-resistance and translucency by acceleration of crystallization using nucleating agents. *Preprints of Seikei-Kakou Autumnal Meeting 2011* **19,** 397–398 (2011).
9 Wo, D. L. & Tanner, R. I. The impact of blue organic and inorganic pigments on the crystallization and rheological properties of isotactic polypropylene. *Rheol. Acta.* **49,** 75–88 (2010).
10 Sterzynski, T., Calo, P. & Thomas, M. *Trans*- and *dimethyl* quinacridone nucleation of isotactic polypropylene. *Polym. Eng. Sci.* **37,** 1917–1927 (1997).
11 Vijayakumar, R. P., Khakhar, D. V. & Misra, A. Phase transformation and enhancement of toughness in polyvinylidene fluoride by onium salts. *J. Polym. Sci. B: Polym. Phys.* **49,** 1339–1344 (2011).
12 Müller, M., Dinnebier, R. E., Jansen, M., Wiedemann, S. & Plüg, C. The influence of temperature, additives and polymorphic form on the kinetics of the phase transformations of copper phthalocyanine. *Dye. Pigment.* **85,** 152–161 (2010).
13 Ashida, M., Uyeda, N. & Suito, E. Unit cell metastable-form constants of various phthalocyanines. *Bull. Chem. Soc. Jpn.* **39,** 2616–2624 (1966).
14 Brown, C. J. Crystal structure of β-copper phthalocyanine. *J. Chem. Soc. A* 2488–2493 (1968).
15 Berger, O., Fischer, W. J., Adolphi, B. & Tierbach, S. Studies on phase transformations of Cu-phthalocyanine thin films. *J. Mat. Sci.: Mat. Elecron.* **11,** 331–346 (2000).
16 Takahashi, Y., Sato, T. & Tadokoro, H. Crystal structure of α-gutta percha: modification of the constrained least-squares method. *J. Polym. Sci.: Polym. Phys. Ed.* **11,** 233–248 (1973).
17 Pan, P., Liang, Z., Cao, A. & Inoue, Y. Layered metal phosphonate reinforced poly(L-lactide) composites with a highly enhanced crystallization rate. *Appl. Mater. Interfaces* **1,** 402–411 (2009).
18 Mathieu, C., Thierry, A., Wittmann, J. C. & Lotz, B. Specificity and versatility of nucleating agents toward isotactic polypropylene crystal phases. *J. Polym. Sci. B: Polym. Phys.* **40,** 2504–2515 (2002).
19 Sun, Y., Li, H., Huang, Y., Chen, E., Zhao, L., Gan, Z. & Yan, S. Epitaxial crystallization of poly(butylene adipate) on highly oriented polyethylene thin film. *Macromolecules* **38,** 2739–2743 (2005).